Downlink Subchannel and Power Allocation in Multi-Cell OFDMA Cognitive Radio Networks

Kae Won Choi, *Member, IEEE*, Ekram Hossain, *Senior Member, IEEE*, and
Dong In Kim, *Senior Member, IEEE*

***Abstract*—We propose a novel subchannel and transmission power allocation scheme for multi-cell orthogonal frequency-division multiple access (OFDMA) networks with cognitive radio (CR) functionality. The multi-cell CR-OFDMA network not only has to control the interference to the primary users (PUs) but also has to coordinate inter-cell interference in itself. The proposed scheme allocates the subchannels to the cells in a way to maximize the system capacity, while at the same time limiting the transmission power on the subchannels on which the PUs are active. We formulate this joint subchannel and transmission power allocation problem as an optimization problem. To efficiently solve the problem, we divide it into multiple subproblems by using the dual decomposition method, and present the algorithms to solve these subproblems. The resulting scheme efficiently allocates the subchannels and the transmission power in a distributed way. The simulation results show that the proposed scheme provides significant improvement over the traditional fixed subchannel allocation scheme in terms of system throughput.**

***Index Terms*—Cognitive radio (CR), opportunistic spectrum access, orthogonal frequency-division multiple access (OFDMA), multi-cell systems, subchannel allocation, optimization, dual decomposition.**

I. Introduction

A cognitive radio (CR) network opportunistically exploits the frequency bands licensed to the primary users (PUs) but not used by the PUs spatially or temporarily (i.e., spectrum holes), and utilizes them to transmit its own data. A CR network is to be built on top of the legacy wireless networks with the ability to avoid harmful interference to the PUs. Therefore, an underlying wireless technology, particularly the multiple access technique has to be chosen which is suitable for CR networks.

Orthogonal frequency-division multiple access (OFDMA) is a viable multiple access technique for CR networks. With its numerous advantages, the OFDMA technology is adopted by most of the next generation cellular wireless networks, for example, the long-term evolution (LTE) and the worldwide interoperability for microwave access (WiMAX) networks [1]. Besides its advantages in conventional wireless networks, OFDMA also has several benefits which make it a good fit for CR networks [2]. For example, an OFDMA system can turn off subcarriers on which a PU is active, while maintaining the connection via the rest of the subcarriers. OFDMA technology has been incorporated into the IEEE 802.22 wireless regional area network (WRAN) [3] standard for CR networks operating in the TV band.

A CR-OFDMA network can be designed on the basis of the existing researches on non-CR OFDMA networks. There have been numerous studies on conventional OFDMA networks, especially focusing on the subcarrier and power allocation problem in a single-cell scenario. A comprehensive survey on these works can be found in [4]. While the works introduced in [4] only consider single-cell OFDMA systems, some other works investigated the radio resource allocation problem for multi-cell OFDMA networks [5]–[10]. The most crucial issue in a multi-cell OFDMA network is the coordination among multiple cells to efficiently reuse the spectrum [5]. In [6] and [7], the authors proposed power management schemes under the condition that all cells share the same spectrum, i.e., frequency reuse factor (FRF) of one. However, the difficulty with FRF being one is that the mobile stations (MSs) located in the edge of a cell can suffer severe inter-cell interference. The fractional frequency reuse (FFR) schemes (e.g., FRF of three, partial frequency reuse (PFR) [8], and soft frequency reuse (SFR) [9]) can resolve this problem by partitioning the spectrum into multiple subchannels[1] and assigning them to the cells. The system performance can be further enhanced by the adaptive FFR scheme (e.g., [5], [10]) that dynamically assigns the subchannels according to the system environment. Since the interference to the PUs needs to be taken into account when allocating radio resources, it is a non-trivial task to develop an optimal resource allocation scheme for CR-OFDMA networks.

Recently, several studies have been done on resource allocation in single-cell CR-OFDMA networks [11]–[13]. In [11], a power loading algorithm for cognitive radios was proposed that uses the frequency bands adjacent to the PU's bands. In [12], the authors solved a joint power and subchannel allocation problem under interference constraint for each subchannel by means of the dual decomposition technique. In [13], a power and subchannel allocation algorithm was proposed for supporting non-real time services in an OFDM-based CR system. With respect to the multi-cell CR-OFDMA networks, only few works have been done so far. In [14], a resource allocation algorithm for a multi-cell OFDMA network was introduced in the context of CR, where the OFDMA network was considered as the PU network that tries to vacate spectrum bands for a CR network. In [15], a frequency channel and power allocation algorithm was proposed that maximizes the number of subscribers in a multi-cell CR network. However, this work considers a frequency-division multiple access (FDMA) system rather than an OFDMA system.

Unlike the conventional multi-cell networks, the CR network, which coexists with the PU network (Fig. 1), should

[1]A subchannel is defined as a set of consecutive subcarriers.

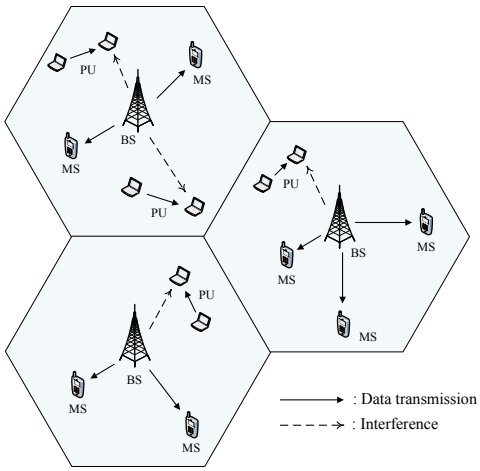

Fig. 1. Co-existence of the CR-OFDMA and PU networks.

control the interference to the PUs as well as the inter-cell interference within the CR network. In this paper, we propose a novel transmission power and subchannel allocation scheme for downlink transmission in multi-cell CR-OFDMA networks with the adaptive FFR strategy. The proposed scheme maximizes the throughput of the CR network by efficiently allocating subchannels to cells, while controlling the interference to the PUs by limiting the transmission power on the subchannels occupied by the PUs. To develop the proposed scheme, we formulate the resource allocation problem as an optimization problem. Then we relax some constraints and decompose the problem into multiple subproblems by using the dual decomposition technique [16]. The proposed scheme significantly outperforms the traditional fixed subchannel allocation scheme (e.g., the static FFR with the FRF of three in [5]). By using simulations, we show that the proposed scheme enhances the system throughput by up to 50% for the same amount of interference to PUs. In addition, the proposed scheme can operate distributively with low control overhead.

The rest of the paper is organized as follows. Section II overviews the system model of the CR and the PU networks. In Section III, we analyze the throughput of each MS and the interference to PUs for given transmission power and subchannel allocation in the CR-OFDMA network. Based on these analytical results, we formulate the optimization problem and present the algorithm to solve it in Section IV. In Section V, we show representative numerical results. Section VI concludes the paper. A list of the key mathematical symbols used in this paper is given in Table I.

II. System Model and the Proposed Resource Allocation Architecture

A. Primary User and Secondary User Network Models

We consider downlink transmission in a multicell CR-OFDMA network as shown in Fig. 1. The CR-OFDMA network consists of M cells, each of which is managed by a base station (BS). Each cell and the corresponding BS are indexed by $m = 1, \ldots, M$. There are total N mobile stations (MSs), each indexed by $n = 1, \ldots, N$. An MS is associated

TABLE I
Table of Symbols

Symbol	Definition
M	Number of cells in the CR network
N	Number of MSs in the CR network
$\mathcal{N}_m$	Set of the MSs in cell m
β_n	Serving BS of MS n
K	Number of subchannels
W	Bandwidth of a subchannel
T_S	Length of a slot
N_o	Noise spectral density
R	Product of the number of the subcarriers in a subchannel and the OFDM symbol rate
$n^*_{k,m}(t)$	MS scheduled by BS m to use subchannel k in slot t
$p_{k,m}$	Transmission power of BS m on subchannel k
$p^{\text{BS}}_{\text{max}}$	Maximum total transmission power of a BS
$s_{k,m}$	Subchannel allocation indicator of BS m on subchannel k
$\mathcal{G}$	Conflict graph
A	Number of all cliques in the conflict graph $\mathcal{G}$
$\mathcal{C}_a$	Set of the indices of all the vertices in clique a
L	Number of all PUs
$\theta^{\text{PU}}_{\text{max}}$	Maximum transmission distance of a PU-Tx
$\mathcal{L}_k$	Set of the PUs using subchannel k
p^{PU}_l	Transmission power of PU-Tx l
$p^{\text{PU}}_{\text{min}}$	Minimum transmission power of a PU-Tx
$I^{\text{PU}}_l(t)$	Total interference from all BSs to PU-Rx l in slot t
$I^{\text{PU}}_{\text{lim}}$	Limit on the interference to a PU-Rx
ϵ	Limit on the interference violation probability
$g^{\text{BS,MS}}_{k,m,n}(t)$	Channel gain from BS m to MS n on subchannel k in slot t
$g^{\text{BS,PU}}_{k,m,l}(t)$	Channel gain from BS m to PU-Rx l on subchannel k in slot t
$g^{\text{PU,BS}}_{k,l,m}(t)$	Channel gain from PU-Tx l to BS m on subchannel k in slot t
$g^{\text{PU,MS}}_{k,l,n}(t)$	Channel gain from PU-Tx l to MS n on subchannel k in slot t
$I^{\text{MS}}_{k,n}(t)$	Interference inflicted on MS n on subchannel k in slot t
$\mathcal{L}_{k,m}$	Set of the PUs using subchannel k and within the cell coverage area of BS m
T_E	Length of a quiet period
$\xi_{k,m}(t)$	Sensing result on subchannel k, produced by BS m in slot t
$\gamma_{k,n}(t)$	SINR of MS n on subchannel k in slot t
$\alpha_{k,n}(t)$	Normalized SINR of MS n on subchannel k in slot t
$r_{k,n}(s,p)$	Average data rate of MS n on subchannel k when the subchannel allocation indicator and the transmission power of the serving BS on subchannel k is s and p, respectively
b_n	Throughput of MS n
$U(x)$	Utility function
$D_{k,m}$	Transmission power limit of BS m on subchannel k

with one serving BS, denoted by β_n. Let $\mathcal{N}_m$ be the set of the MSs associated with BS m (i.e., the MSs in cell m). An MS communicates with the serving BS by using the OFDMA technique in which consecutive subcarriers are bundled into a subchannel. Let W denote the bandwidth of a subchannel, and let K denote the number of subchannels. Each subchannel is indexed by $k = 1, \ldots, K$. We consider a slotted system, where the length of a slot is denoted by T_S. A slot can contain one or more OFDMA symbols. Each slot is indexed by t. One subchannel during one slot constitutes a resource block (RB). For each cell, an RB can be allocated to only one MS, which is selected by the scheduler residing in the BS. An opportunistic scheduling algorithm is used, which selects the MS in a relatively good instantaneous channel condition. Let $n^*_{k,m}(t)$ denote the MS scheduled[2] by BS m to use subchannel k in slot t. Let $p_{k,m}$ denote the transmission power of BS m on subchannel k.[3] The maximum total transmission power of a BS is denoted by $p^{\text{BS}}_{\max}$. Then, the following inequality should hold: $\sum_{k=1}^{K} p_{k,m} \le p^{\text{BS}}_{\max}$ for $m = 1, \ldots, M$.

If BS m schedules MS n on subchannel k in slot t (i.e., $n^*_{k,m}(t) = n$), it transmits to MS n with the transmission power of $p_{k,m}$. The signal-to-interference-plus-noise ratio (SINR) at MS n in slot t is given by:

$$\gamma_{k,n}(t) := \frac{g^{\text{BS,MS}}_{k,\beta_n,n}(t) \cdot p_{k,\beta_n}}{I^{\text{MS}}_{k,n}(t) + N_o W} \tag{1}$$

where $g^{\text{BS,MS}}_{k,m,n}(t)$ is the channel gain from BS m to MS n on subchannel k in slot t, N_o is the noise spectral density, and $I^{\text{MS}}_{k,n}(t)$ is the interference to MS n on subchannel k in slot t from the PUs and the BSs other than the serving BS. Then the instantaneous data rate of MS n is given by: $R \log_2(1 + \gamma_{k,n}(t))$, where R denotes the product of the number of the subcarriers in a subchannel and the OFDM symbol rate.

The CR network coexists with the PU network. The PUs communicate over point-to-point links (Fig. 1). There are L pairs of PU transmitters (PU-Tx's) and PU receivers (PU-Rx's). Each pair of a PU-Tx and a PU-Rx is indexed by $l = 1 \ldots, L$. A PU-Rx is located within the maximum transmission distance, denoted by $\theta^{\text{PU}}_{\max}$, from the corresponding PU-Tx. PU-Tx l transmits signals to PU-Rx l via one subchannel. Let $\mathcal{L}_k$ denote the set of the PUs using subchannel k. The transmission power of PU-Tx l is denoted by p^{PU}_l. It is assumed that the transmission power of a PU-Tx is no less than $p^{\text{PU}}_{\min}$ (i.e., $p^{\text{PU}}_l \ge p^{\text{PU}}_{\min}$). We assume that the subchannel usage and the transmission power of the PUs change slowly. Even though we assume the point-to-point communication for the PU networks for ease of presentation, this PU network model can easily be extended to more generic one by allowing that several PU-Tx's or PU-Rx's can be located within the same wireless node. For example, we can place all PU-Tx's on the center node while putting each PU-Rx on a separate node around the center node in order to describe a star topology network.

The scenario where the CR network is a multicell OFDMA network and the PU network is a distributive network consisting of point-to-point links is of practical importance. The IEEE 802.22-based WRAN [3] standard defines a license-exempt cellular-based OFDMA network operating in the VHF/UHF TV bands on a non-intrusive basis. Other than TV receivers, the PUs in the VHF/UHF TV bands include a wireless microphone, the primary application of which is transmitting an audio signal over a short distance. Another example can be the IEEE 802.16h License-Exempt (LE) that is an amendment of the IEEE 802.16 standard for the improved coexistence mechanisms for license-exempt operation [18].

We consider a spectrum underlay CR (e.g., [19]), in which CR-BSs are permitted to transmit signals on the same subchannel with PUs as long as the interference is kept under a tolerable level. Let $g^{\text{BS,PU}}_{k,m,l}(t)$ denote the channel gain from BS m to PU-Rx l on subchannel k in slot t. Then, the total interference from all BSs to PU-Rx l in slot t is given by $I^{\text{PU}}_l(t) := \sum_{m=1}^{M} g^{\text{BS,PU}}_{k,m,l}(t) \cdot p_{k,m}$, if PU l uses subchannel k (i.e., $l \in \mathcal{L}_k$). Let $I^{\text{PU}}_{\text{lim}}$ denote the limit on the interference to a PU-Rx. We define the interference violation probability as the probability that the total interference to a PU-RX, $I^{\text{PU}}_l(t)$, exceeds the limit on the interference, $I^{\text{PU}}_{\text{lim}}$. The CR network should maintain the interference violation probabilities of PUs under the given threshold, ϵ. That is,

$$\Pr[I^{\text{PU}}_l(t) > I^{\text{PU}}_{\text{lim}}] \le \epsilon, \quad \forall l = 1, \ldots, L. \tag{2}$$

To satisfy the above constraints, each CR-BS m limits the transmission power, $p_{k,m}$, to the transmission power limit, $D_{k,m}$, for all subchannels (i.e., $p_{k,m} \le D_{k,m}$ for $k = 1, \ldots, K$). For maximum performance of the CR network, the transmission power limits should be set as high as possible within the range that makes the constraints on the interference violation probabilities satisfied. The method to determine the transmission power limit based on an energy detection-based channel sensing method [20] will be described in Section III-B.

The channel gain of a wireless link between two nodes (e.g., $g^{\text{BS,MS}}_{k,m,l}(t)$ and $g^{\text{BS,PU}}_{k,m,l}(t)$) on a subchannel in slot t is: $g(t) = \rho(d) \cdot 10^{\psi(t)/10} \cdot \omega(t)$, where $\rho(d)$ is the path-loss for distance d between two nodes, $10^{\psi(t)/10}$ is the lognormal shadow fading component, and $\omega(t)$ is the multi-path Rayleigh fading component of channel gain. The shadowing and multi-path fading processes are assumed to be stationary. Here $\psi(t)$ follows a normal distribution with the mean of zero and the standard deviation of σ_ψ. The multi-path fading $\omega(t)$ follows an exponential distribution with the mean of μ_ω. We assume that the channel gains of two different wireless links are statistically independent.

B. Subchannel Coordination Strategy for Frequency Reuse in the Multi-Cell CR-OFDMA Network

To reduce inter-cell interference, several variants of the FFR strategy can be used. Among them, the simplest one is to allocate subchannels to cells for their exclusive use. Once a subchannel is allocated to a cell, the nearby cells are not allowed to use the subchannel. Let $s_{k,m}$ be the "subchannel allocation indicator" of subchannel k on BS m: $s_{k,m} = 1$ if the

[2]We will explain the scheduling algorithm in detail in Section III-A.

[3]We assume that a BS does not adjust the transmission power in a fast time scale. It is known (e.g., in [17]) that the fixed power allocation scheme can show near-optimal performance in a multi-user OFDMA network.

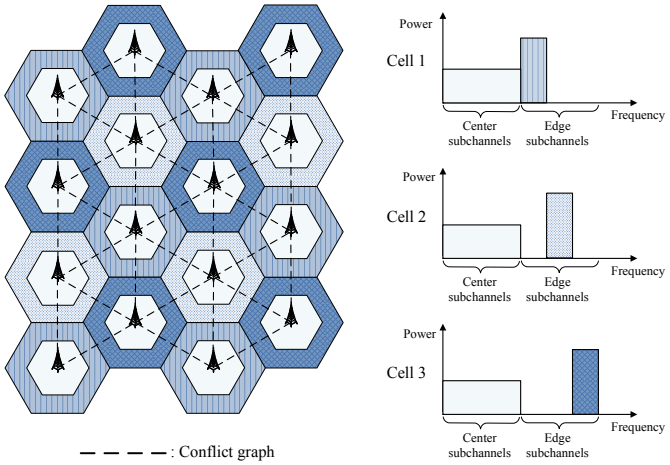

Fig. 2. The conflict graph and the partial frequency reuse (PFR) scheme.

subchannel k is allocated to cell m; $s_{k,m} = 0$, otherwise. A BS can transmit power on a subchannel only when the subchannel is allocated to the BS. That is, $p_{k,m} = 0$ if $s_{k,m} = 0$. Since one subchannel cannot be allocated to two adjacent cells at the same time, $s_{k,i}$ and $s_{k,j}$ cannot be both one at the same time in the case that cell i and cell j are close to each other.

To represent the geographical relationship between cells, we introduce the "conflict graph" $\mathcal{G} := (\mathcal{V}, \mathcal{E})$. In the conflict graph $\mathcal{G}$, there are M vertices (i.e., $|\mathcal{V}| = M$) and vertex $v_m \in \mathcal{V}$ stands for cell m. There exists an edge (i, j) in $\mathcal{E}$, if and only if cell i and cell j are close enough to interfere with each other.[4] In Fig. 2, we present an example of the conflict graph. A clique in a graph is defined as a subset of $\mathcal{V}$ such that there is an edge between every two vertices in the clique. The number of all cliques in the graph $\mathcal{G}$ is denoted by A, and each clique is indexed by $a = 1, \ldots, A$. Let $\mathcal{C}_a$ denote the set of the indices of all the vertices in clique a. Cells do not interfere with each other if and only if the following condition is met:

$$\sum_{m \in \mathcal{C}_a} s_{k,m} \leq 1, \quad \forall k = 1, \ldots, K \quad \text{and} \quad \forall a = 1, \ldots, A. \quad (3)$$

The proposed resource allocation scheme is a type of dynamic FFR strategy [5], that adaptively decides the subchannel allocation indicator, $s_{k,m}$, under the constraint in (3). The use of the subchannel allocation indicator can be regarded as a suboptimal simplification, since it forces the transmission powers of some BSs to be zero for interference management. The computational complexity and the control message overhead between BSs can be reduced significantly by introducing the subchannel allocation indicator.

The proposed resource allocation architecture can also be used along with the the partial frequency reuse (PFR) strategy [8]. The PFR strategy allows the nearby cells to use the same subchannel only for the MSs close to their serving BSs. The basic concept of the PFR strategy is illustrated in Fig. 2. The entire frequency band is divided into center subchannels and edge subchannels as in Fig. 2. While the center subchannels can be used by all cells at the same time, the edge subchannels are allocated to some cells for their exclusive use. The MSs close to the serving BS (i.e., the center MSs) can make use of both the center and edge subchannels. On the other hand, the MSs located relatively far from the serving BS (i.e., the edge MSs) can only utilize the edge subchannels for protection from inter-cell interference. The proposed scheme can be used to solve the resource allocation problem in the edge subchannels, while the resource allocation problem in the center subchannels can independently be solved by each cell by using the algorithms for single-cell CR-OFDMA systems (e.g., [12]). When the proposed scheme is applied to the PFR strategy, we redefine the subchanels $1, \ldots, K$ as the edge subchannels, the MSs $1, \ldots, N$ as the edge MSs and the center MSs having permission to use the edge subchannels, and the maximum total transmission power of a BS, $p_{\max}^{\text{BS}}$, as the transmission power dedicated to the edge subchannels.

[4]Strictly speaking, cell i interferes with cell j when BS i using its maximum transmission power can possibly interfere with any MS in the coverage area of cell j.

C. Overall Resource Allocation Architecture

We develop a subchannel and transmission power allocation scheme that aims to accomplish the following three goals: 1) The transmission power should be allocated in such a way to limit the interference on PUs. The BSs should restrict the transmission power on the subchannels where a strong PU signal is detected. 2) The BSs should efficiently allocate the subchannels to maximize the system capacity. A subchannel should be allocated to the cell around which there is no PU using the subchannel. 3) Fairness should be guaranteed among MSs. More radio resources should be allocated to cells accommodating more MSs in order to provide fairness over the entire network. To achieve these goals, we first formulate an optimization problem. Then, this optimization problem is decomposed into three subproblems corresponding to these three goals. By solving these subproblems, we can accomplish the corresponding goals.

The algorithms to solve the subproblems are assigned to the respective functional blocks in a BS, namely, the fairness control block, the transmission power allocation block, and the subchannel allocation block, as shown in Fig. 3. We will explain the detailed algorithms in the functional blocks in Section IV. The fairness control block allocates more radio resources to the BS if the data rate provided to the MSs in the corresponding cell is not sufficient. The transmission power allocation block allocates transmission power to each subchannel in such a way that the transmission power is limited in the subchannels with the PU signal detected. The subchannel allocation block plays a key role in maximizing the system performance. Suppose that the distribution of MSs within a cell is the same for all cells. If the subchannel allocation block assigns a subchannel to the BS for which the transmission power limit on the subchannel is relatively high, the BS is able to transmit high transmission power on that subchannel. Then, this BS can make better use of the subchannel than the other BSs can. The subchannel allocation block in a BS works with the subchannel allocation blocks in the other BSs.

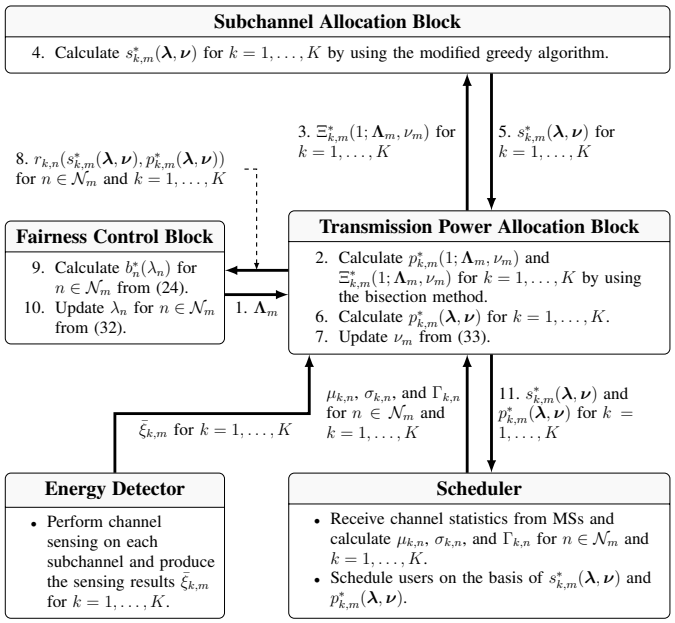

Fig. 3. Algorithms for solving the decomposed problems in the functional block structure (for BS m).

The numbers of MSs and their association to BS (i.e., N and β_n), the transmission power and the channel usage of PUs (i.e., p_l^{PU} and $\mathcal{L}_k$), and the path-loss component in the channel gain vary slowly enough so that they can be treated as fixed during the resource allocation interval. On the other hand, the shadowing and multi-path fading components in the channel gain vary in a faster time scale. The opportunistic scheduler in a BS responds to fast variation in a channel gain and schedules an MS (i.e., $n^*_{k,m}(t)$) on a slot-by-slot basis. However, subchannel and transmission power allocation (i.e., $s_{k,m}$ and $p_{k,m}$) are performed in a slower time scale, for example, in response only to the changes in the MS and PU configuration, not to the instantaneous channel condition.

III. Intra-Cell Scheduling and Interference Management

In Section III-A, we analyze the average data rates of MSs when an opportunistic scheduling algorithm is applied for the given transmission power and subchannel allocation. In Section III-B, we explain how to determine the transmission power limits based on the sensing results from the energy detector. The results from both sections will be used in Section IV to formulate the multi-cell resource allocation problem.

A. Throughput Analysis of Opportunistic Scheduling Algorithm and Utility of an MS

Let $r_{k,n}(s,p)$ denote the average data rate of MS n on subchannel k when the subchannel allocation indicator and the transmission power of the serving BS on the subchannel k are s and p, respectively (i.e., $s_{k,\beta_n}=s$ and $p_{k,\beta_n}=p$). Clearly, we have $r_{k,n}(s,p)=0$ when $s=0$. We will now derive an analytical expression for $r_{k,n}(s,p)$ for $s=1$.

In each slot t for each subchannel k, the scheduler selects MS $n^*_{k,m}(t)$ and decides the data rate for the selected MS, based on the SINR reported from the MSs in the cell.[5] We use the SINR-based proportional fair (PF) scheduling algorithm [21] to select an MS for an RB. Recall that $\gamma_{k,n}(t)$ denotes the SINR of MS n on subchannel k. An RB of cell m on the subchannel k in slot t is allocated to MS $n^*_{k,m}(t)$ such that $n^*_{k,m}(t)\in\text{argmax}_{n\in\mathcal{N}_m}\alpha_{k,n}(t)$, where $\alpha_{k,n}(t):=\gamma_{k,n}(t)/\,\text{E}[\gamma_{k,n}(t)]$ is the normalized SINR of MS n on subchannel k in slot t.

We calculate the scheduling probability for the above scheduling rule, and then derive the average data rate from this probability. Since MS n is scheduled if it has the highest normalized SINR among the MSs in its serving cell, the probability that MS n with the normalized SINR of x is scheduled is $\prod_{\substack{i\in\mathcal{N}_{\beta_n}\\ i\neq n}}F_{\alpha_{k,i}}(x)$, where $F_{\alpha_{k,i}}$ is the cumulative density function (cdf) of $\alpha_{k,i}(t)$. We can derive $r_{k,n}(1,p)$ as in (4), where $\Gamma_{k,n}:=\text{E}[\gamma_{k,n}(t)]/p_{k,\beta_n}=\text{E}[g^{\text{BS,MS}}_{k,\beta_n,n}(t)/(I^{\text{MS}}_{k,n}(t)+N_oW)]$, and $f_{\alpha_{k,n}}$ is the probability density function (pdf) of $\alpha_{k,n}(t)$.

To evaluate (4), we require to know the distribution of the normalized SINR. In (1), we have $I^{\text{MS}}_{k,n}(t)=\sum_{\substack{m=1,\ldots,M\\ m\neq\beta_n}}g^{\text{BS,MS}}_{k,m,n}(t)\cdot p_{k,m}+\sum_{l\in\mathcal{L}_k}g^{\text{PU,MS}}_{k,l,n}(t)\cdot p^{\text{PU}}_{k,l}$, where $g^{\text{PU,MS}}_{k,l,n}(t)$ denotes the channel gain from PU-Tx l to MS n on subchannel k in slot t. Since we consider the case that subchannel k is allocated to the serving BS (i.e, $s_{k,\beta_n}=1$) in order to calculate $r_{k,n}(s,p)$ for $s=1$, the subchannel allocation indicators and the transmission powers of the nearby BSs are zero (i.e., due to the constraints in (3)). Thus, we have $\sum_{\substack{m=1,\ldots,M\\ m\neq\beta_n}}g^{\text{BS,MS}}_{k,m,n}(t)\cdot p_{k,m}\simeq 0$, if the interferences from the BSs other than the nearby BSs are assumed to be zero (i.e., due to distance). Then, the normalized SINR can be written as

$$\alpha_{k,n}(t)=\frac{g^{\text{BS,MS}}_{k,\beta_n,n}(t)}{\Gamma_{k,n}\cdot\left(\sum_{l\in\mathcal{L}_k}g^{\text{PU,MS}}_{k,l,n}(t)\cdot p^{\text{PU}}_{k,l}+N_oW\right)}. \quad (5)$$

The composite lognormal and exponential distribution of $g^{\text{BS,MS}}_{k,m,n}(t)$ and $g^{\text{PU,MS}}_{k,l,n}(t)$ approximately follows a purely lognormal distribution [22].[6] Then, the numerator in (5) becomes lognormally distributed. In addition, since N_oW is a deterministic variable, the denominator in (5) can be approximated by another lognormal distribution.[7] The numerator and the denominator in (5) are independent of each other since the channel gain between MS n and the serving BS (i.e., $g^{\text{BS,MS}}_{k,\beta_n,n}(t)$) is independent of the channel gain between MS n and PU l (i.e., $g^{\text{PU,MS}}_{k,l,n}(t)$) for all l. Since both the numerator and the denominator in (5) are lognormally distributed and

[5] We do not require to consider the interference to PU-Rx's for the scheduling algorithm. Since the downlink of the CR-OFDMA system is assumed, the transmitting end of a wireless link is always a BS, not an MS. Therefore, the interference to PU-Rx's is not affected by which MS is selected by the scheduler.

[6] This lognormal approximation holds when the composite distribution is mainly dominated by the lognormal distribution. Since the standard deviation of the shadow fading component, $\psi(t)$, is generally very large (i.e., $\sigma_\psi=8$ dB), this approximation can be justified [22], [23].

[7] The sum of independent lognormal distributions can well be approximated by another lognormal distribution [24].

$$r_{k,n}(1,p) = \int_0^\infty R\log_2(1+p\cdot\Gamma_{k,n}\cdot x)\cdot\left\{\prod_{i\in\mathcal{N}_{\beta_n},i\neq n} F_{\alpha_{k,i}}(x)\right\}\cdot f_{\alpha_{k,n}}(x)\cdot dx. \quad (4)$$

independent of each other, the normalized SINR follows a lognormal distribution. Then, the logarithm of $\alpha_{k,n}(t)$ (i.e., $10\log_{10}\alpha_{k,n}(t)$) follows normal distribution with mean of $\mu_{k,n}$ and standard deviation of $\sigma_{k,n}$.

To calculate $r_{k,n}(1,p)$, the serving BS should be aware of $\mu_{k,n}$, $\sigma_{k,n}$, and $\Gamma_{k,n}$. The serving BS can calculate these values from the statistics of the channel gain between MS n and the serving BS in dB (i.e., $\chi_{k,n}(t) := 10\log_{10} g^{\text{BS,MS}}_{k,\beta_n,n}(t)$) and the noise plus interference in dB (i.e., $\kappa_{k,n}(t) := 10\log_{10}(\sum_{l\in\mathcal{L}_k} g^{\text{PU,MS}}_{k,l,n}(t)\cdot p^{\text{PU}}_{k,l} + N_oW)$). Since the statistical characteristics of $\chi_{k,n}(t)$'s are the same for all subchannels, MS n can estimate $\text{E}[\chi_{k,n}(t)]$ and $\text{Var}[\chi_{k,n}(t)]$ from pilot symbols on any subchannel. Also, MS n can estimate $\text{E}[\kappa_{k,n}(t)]$ and $\text{Var}[\kappa_{k,n}(t)]$ when BSs perform energy detection. From these statistics reported from MS n, the serving BS calculates $\mu_{k,n} = -\frac{\ln 10}{20}(\text{Var}[\chi_{k,n}(t)] + \text{Var}[\kappa_{k,n}(t)])$, $\sigma_{k,n} = \sqrt{\text{Var}[\chi_{k,n}(t)] + \text{Var}[\kappa_{k,n}(t)]}$, and $\Gamma_{k,n} = \exp(\frac{\ln 10}{10}(\text{E}[\chi_{k,n}(t)] - \text{E}[\kappa_{k,n}(t)] + \frac{\ln 10}{20}(\text{Var}[\chi_{k,n}(t)] + \text{Var}[\kappa_{k,n}(t)])))$. Then, the pdf and the cdf of the normalized SINR are

$$f_{\alpha_{k,n}}(x) = \frac{10/\ln 10}{x\sigma_{k,n}\sqrt{2\pi}}\exp\left(-\frac{(10\log_{10}x-\mu_{k,n})^2}{2\sigma^2_{k,n}}\right) \quad (6)$$

$$F_{\alpha_{k,n}}(x) = 1 - \frac{1}{2}\,\text{erfc}\left(\frac{10\log_{10}x-\mu_{k,n}}{\sqrt{2}\sigma_{k,n}}\right) \quad (7)$$

where erfc is the complementary error function, defined as $\text{erfc}(x) = 2/\sqrt{\pi}\int_x^\infty \exp(-t^2)dt$.

With infinite backlog at the MSs, if we let b_n denote the throughput of MS n, we have $b_n \le \sum_{k=1}^K r_{k,n}(s_{k,\beta_n}, p_{k,\beta_n})$, and the utility of MS n is defined as [25]:

$$U(x) := \begin{cases}\log b_n, & \text{if } \zeta = 1\\ (1-\zeta)^{-1}{b_n}^{(1-\zeta)}, & \text{otherwise}\end{cases} \quad (8)$$

where $\zeta \ge 0$ determines the fairness. The higher the value of ζ, the more fairness we can ensure at the cost of efficiency. The fairness among the MSs can be achieved by maximizing $\sum_{n=1}^N U(b_n)$.

B. Estimation of Interference to Primary Users for Calculating Transmission Power Limits

In this section, we explain how to decide the transmission power limits based on the sensing results from the energy detector. Each BS is responsible to protect only PU-Rx's within its cell coverage area, since the interference from a BS to the PU-Rx's out of its cell coverage area is very small. With a slight abuse of notation, let $\mathcal{L}_{k,m}$ denote the set of PU-Rx's using subchannel k and within the cell coverage area of BS m. Consider a PU-Rx l such that $l \in \mathcal{L}_{k,m}$. BS m should protect such PU-Rx l when subchannel k is allocated to itself (i.e., $s_{k,m} = 1$). If $s_{k,m} = 1$, the subchannel allocation indicators and the transmission powers of the BSs neighboring BS m become zero, and therefore, PU-Rx l only receives the interference from BS m and distant BSs. Since the interference from the distant BSs is negligible, the total interference to PU-Rx l is given by $I^{\text{PU}}_l(t) = \sum_{i=1}^M g^{\text{BS,PU}}_{k,i,l}(t)\cdot p_{k,i} \simeq g^{\text{BS,PU}}_{k,m,l}(t)\cdot p_{k,m}$, for $l \in \mathcal{L}_{k,m}$ when $s_{k,m} = 1$.

Now, we derive the distribution of the interference and calculate the interference violation probability. According to [22], the logarithm of $g^{\text{BS,PU}}_{k,m,l}(t)$ (i.e., $10\log_{10} g^{\text{BS,PU}}_{k,m,l}(t)$) approximately follows a normal distribution with the mean of $10\log_{10}\rho(d^{\text{BS,PU-Rx}}_{m,l}) + 10\log_{10}\mu_\omega - 2.5$ and the standard deviation of $\sqrt{\sigma^2_\psi + 5.57^2}$, where $d^{\text{BS,PU-Rx}}_{m,l}$ is the distance from BS m to PU-Rx l. Provided that $I^{\text{PU}}_l(t) = g^{\text{BS,PU}}_{k,m,l}(t)\cdot p_{k,m}$, we can calculate the interference violation probability of PU l as in (9), where $Q(x) := 1/\sqrt{2\pi}\int_x^\infty \exp(-\frac{u^2}{2})du$.

Since the interference violation probability should be less than ϵ (i.e., $\Pr[I^{\text{PU}}_l(t) > I^{\text{PU}}_{\text{lim}}] \le \epsilon$), we have the restriction on the transmission power such that $p_{k,m} \le \Phi(d^{\text{BS,PU-Rx}}_{m,l})$, where $\Phi(d) := \frac{I^{\text{PU}}_{\text{lim}}}{\rho(d)\cdot\mu_\omega}\cdot 10^{0.25-0.1\sqrt{\sigma^2_\psi+5.57^2}\cdot Q^{-1}(\epsilon)}$. To satisfy this restriction for all $l \in \mathcal{L}_{k,m}$, we set the transmission power limit $D_{k,m}$ to $\Phi(d)$ for d that is a lower bound of the distance from BS m to PU-Rx's such that $d \le d^{\text{BS,PU-Rx}}_{m,l}$ for all $l \in \mathcal{L}_{k,m}$. A BS derives such a lower bound by using the sensing results from the energy detector.

Let us describe the operation of the energy detector. During a channel sensing period (e.g., quiet period in 802.22 WRAN), the length of which is denoted by T_E, the energy detector takes WT_E baseband complex signal samples on each subchannel. Let $y_{k,m,i}(t)$ denote the ith signal sample on subchannel k at BS m in a quiet period in slot t. The energy detector calculates the sensing result $\xi_{k,m}(t) = \frac{2}{N_o}\sum_{i=1}^{WT_E}|y_{k,m,i}(t)|^2$. The power received from all PU-Tx's using subchannel k in slot t is $\sum_{l\in\mathcal{L}_k} g^{\text{PU,BS}}_{k,l,m}(t)\cdot p^{\text{PU}}_{k,l}$, where $g^{\text{PU,BS}}_{k,l,m}(t)$ is the channel gain from PU-Tx l to BS m on subchannel k in slot t. According to [20], $\xi_{k,m}(t)$ follows a noncentral chi-square distribution with $2WT_E$ degrees of freedom and the noncentrality parameter of $\frac{2T_E}{N_o}\sum_{l\in\mathcal{L}_k} g^{\text{PU,BS}}_{k,l,m}(t)\cdot p^{\text{PU}}_{k,l}$, given $g^{\text{PU,BS}}_{k,l,m}(t)$'s for all l. The BS calculates the sensing results over a number of channel sensing periods and takes an average of these sensing results. If the number of the sensing results is sufficiently large, the variation due to the lognormal shadow fading, the Rayleigh fading, and the thermal noise can be averaged out. Then, the BS can have the average sensing result $\bar{\xi}_{k,m} \simeq \text{E}[\xi_{k,m}(t)] = 2WT_E + \frac{2T_E}{N_o}\sum_{l\in\mathcal{L}_k}\text{E}[g^{\text{PU,BS}}_{k,l,m}(t)]\cdot p^{\text{PU}}_{k,l}$.

From the average sensing result, we derive a lower bound of the distance from BS m to PU-Rx's. Let $d^{\text{BS,PU-Tx}}_{m,l}$ denote the distance between BS m and PU-Tx l. Then, we have $\text{E}[g^{\text{PU,BS}}_{k,l,m}(t)] = \rho(d^{\text{BS,PU-Tx}}_{m,l})\cdot\text{E}[10^{\psi(t)/10}]\cdot\text{E}[\omega(t)] = \rho(d^{\text{BS,PU-Tx}}_{m,l})\cdot 10^{\frac{\ln 10}{200}\cdot\sigma^2_\psi}\cdot\mu_\omega$. The distance $d^{\text{BS,PU-Tx}}_{m,l}$ can be calculated as $d^{\text{BS,PU-Tx}}_{m,l} = \rho^{-1}(\text{E}[g^{\text{PU,BS}}_{k,l,m}]/(10^{\frac{\ln 10}{200}\cdot\sigma^2_\psi}\cdot\mu_\omega))$. Also, recall that $\theta^{\text{PU}}_{\text{max}}$ denotes the maximum distance from a PU-Tx to the corresponding PU-Rx. Then, we can calculate

$$\Pr[I_l^{\text{PU}}(t) > I_{\text{lim}}^{\text{PU}}] = \Pr[10\log_{10} I_l^{\text{PU}}(t) > 10\log_{10} I_{\text{lim}}^{\text{PU}}]$$
$$= Q\Big(\frac{10\log_{10} I_{\text{lim}}^{\text{PU}} - 10\log_{10}\rho(d_{m,l}^{\text{BS,PU-Rx}}) - 10\log_{10}\mu_\omega + 2.5 - 10\log_{10} p_{k,m}}{\sqrt{\sigma_\psi^2 + 5.57^2}}\Big). \quad (9)$$

the lower bound of the distance from BS m to PU-Rx l for all $l \in \mathcal{L}_k$ as in (10), where $[x]^+ = \max\{0, x\}$ and $d_{\text{min}}^{\text{BS,PU-Rx}}(\bar{\xi})$ is the lower bound of the distance from a BS to a PU-Rx given the average sensing result $\bar{\xi}$. This lower bound can be viewed as a conservative estimate of the distance to the nearest PU-Rx, derived by assuming the worst-case scenario. Note that the equality in (10) holds when i) there is one PU-Tx around BS m; ii) the corresponding PU-Rx is located at the position closest to BS m within the transmission range of the PU-Tx; and iii) the PU-Tx transmits a signal using the minimum transmission power, $p_{\text{min}}^{\text{PU}}$.

From (10), BS m calculates the transmission power limits from the average sensing results as

$$D_{k,m} = \Phi(d_{\text{min}}^{\text{BS,PU-Rx}}(\bar{\xi}_{k,m})), \qquad \forall k = 1, \ldots, K. \quad (11)$$

This transmission power limit is a conservative one, since it is based on the worst-case estimate of the distance to a PU-Rx. Since a BS can transmit power only on the subchannels allocated to itself, the transmission power $p_{k,m}$ should satisfy the following constraint:

$$0 \le p_{k,m} \le s_{k,m} \cdot D_{k,m}, \quad \forall k \text{ and } \forall m. \quad (12)$$

IV. Inter-Cell Subchannel and Power Allocation Algorithm

A. Subchannel and Transmission Power Allocation Problem

The inter-cell subchannel and transmission power allocation problem can now be formulated as follows:

$$\max_{\mathbf{b},\bar{\mathbf{s}},\bar{\mathbf{p}}} \quad \sum_{n=1}^{N} U(b_n) \quad (13)$$

$$\text{s.t.} \quad b_n \le \sum_{k=1}^{K} r_{k,n}(s_{k,\beta_n}, p_{k,\beta_n}), \quad \forall n = 1, \ldots, N \quad (14)$$

$$b_n \ge 0, \quad \forall n = 1, \ldots, N \quad (15)$$

$$\sum_{k=1}^{K} p_{k,m} \le p_{\text{max}}^{\text{BS}}, \quad \forall m = 1, \ldots, M \quad (16)$$

$$0 \le p_{k,m} \le s_{k,m} \cdot D_{k,m}, \quad \forall k = 1, \ldots, K \text{ and } \forall m = 1, \ldots, M \quad (17)$$

$$\sum_{m \in \mathcal{C}_a} s_{k,m} \le 1, \quad \forall k = 1, \ldots, K \text{ and } \forall a = 1, \ldots, A \quad (18)$$

$$s_{k,m} \in \{0, 1\}, \quad \forall k = 1, \ldots, K \text{ and } \forall m = 1, \ldots, M \quad (19)$$

where $\mathbf{b} := (b_n)_{n=1,\ldots,N}$, $\bar{\mathbf{s}} := (s_{k,m})_{\substack{k=1,\ldots,K \\ m=1,\ldots,M}}$, and $\bar{\mathbf{p}} := (p_{k,m})_{\substack{k=1,\ldots,K \\ m=1,\ldots,M}}$.

We aim to find the subchannel allocation indicator $s_{k,m}$ and the transmission power $p_{k,m}$ that maximize the objective function in this problem. The constraints in (14) and (16) span over entire subchannels. We will relax these constraints by using the Lagrange multipliers to decompose the problem into multiple subproblems. Each subproblem can be solved separately by the functional blocks described in Fig. 3. Among these subproblems, the one related to subchannel allocation is reduced to the well-known combinatorial optimization problem, named the maximum weighted independent set (MWIS) problem. We will propose a suboptimal distributed algorithm to solve the MWIS problem.

The optimization problem in (13) is a mixed binary integer problem which is not a convex optimization problem. However, it is proven in [26] that the duality gap approaches zero as the number of subcarriers increases in the OFDMA system. This is due to the fact that, the time-sharing condition, which generally holds in a time-division multiple access (TDMA) system, is also satisfied in a multicarrier system with a large number of subcarriers. This theorem can also be applied to our optimization problem. We present the proof of zero duality gap in a separate technical report [27]. The number of subchannels in the next generation OFDMA network (e.g., LTE) will be at least 50 in the bandwidth of more than 10 MHz. This number of subchannels is enough to approximately accomplish zero duality gap.

B. Dual Decomposition

To decompose the optimization problem, we relax the constraints in (14) and (16), and then we derive the Lagrangian in (22), where $\boldsymbol{\lambda} := (\lambda_n)_{n=1,\ldots,N}$ and $\boldsymbol{\nu} := (\nu_m)_{m=1,\ldots,M}$ are the Lagrange multipliers, $\boldsymbol{\Lambda}_m := (\lambda_n)_{n \in \mathcal{N}_m}$,

$$\Theta(b_n; \lambda_n) := U(b_n) - \lambda_n b_n \quad (20)$$

and

$$\Xi_{k,m}(s_{k,m}, p_{k,m}; \boldsymbol{\Lambda}_m, \nu_m) := \sum_{n \in \mathcal{N}_m} \lambda_n r_{k,n}(s_{k,m}, p_{k,m}) - \nu_m p_{k,m}. \quad (21)$$

The dual function $h(\boldsymbol{\lambda}, \boldsymbol{\nu})$ can be calculated by maximizing $\Omega(\mathbf{b}, \bar{\mathbf{s}}, \bar{\mathbf{p}}; \boldsymbol{\lambda}, \boldsymbol{\nu})$ as in (23), where $\mathbf{s}_k := (s_{k,m})_{m=1,\ldots,M}$ and the domain is defined by the constraints (15), (17), (18), and (19). As can be seen in (23), we decompose the optimization problem into subproblems 1–3. In addition, we need to solve the dual problem to find the Lagrange multipliers minimizing the dual function.

Now, we define and solve these problems (i.e., subproblems 1–3 and dual problem) one by one.

$$
\begin{aligned}
d_{m,l}^{\text{BS,PU-Rx}} &\geq [d_{m,l}^{\text{BS,PU-Tx}} - \theta_{\max}^{\text{PU}}]^+ = [\rho^{-1}(\mathrm{E}[g_{k,l,m}^{\text{PU,BS}}(t)]/(10^{\frac{\ln 10}{200}\cdot\sigma_\psi^2}\cdot\mu_\omega)) - \theta_{\max}^{\text{PU}}]^+ \\
&\geq \left[\rho^{-1}\left(\frac{\sum_{l\in\mathcal{L}_k}\mathrm{E}[g_{k,l,m}^{\text{PU,BS}}(t)]}{10^{\frac{\ln 10}{200}\cdot\sigma_\psi^2}\cdot\mu_\omega}\right) - \theta_{\max}^{\text{PU}}\right]^+ = \left[\rho^{-1}\left(\frac{\frac{N_o}{2T_E}\bar{\xi}_{k,m} - N_oW}{p_{k,l}^{\text{PU}}\cdot 10^{\frac{\ln 10}{200}\cdot\sigma_\psi^2}\cdot\mu_\omega}\right) - \theta_{\max}^{\text{PU}}\right]^+ \\
&\geq \left[\rho^{-1}\left(\frac{\frac{N_o}{2T_E}\bar{\xi}_{k,m} - N_oW}{p_{\min}^{\text{PU}}\cdot 10^{\frac{\ln 10}{200}\cdot\sigma_\psi^2}\cdot\mu_\omega}\right) - \theta_{\max}^{\text{PU}}\right]^+ = d_{\min}^{\text{BS,PU-Rx}}(\bar{\xi}_{k,m}).
\end{aligned} \tag{10}
$$

$$
\begin{aligned}
\Omega(\mathbf{b},\bar{\mathbf{s}},\bar{\mathbf{p}};\boldsymbol{\lambda},\boldsymbol{\nu}) &:= \sum_{n=1}^{N}U(b_n) + \sum_{n=1}^{N}\lambda_n\left\{\sum_{k=1}^{K}r_{k,n}(s_{k,\beta_n},p_{k,\beta_n}) - b_n\right\} + \sum_{m=1}^{M}\nu_m\left\{p_{\max}^{\text{BS}} - \sum_{k=1}^{K}p_{k,m}\right\} \\
&= \sum_{n=1}^{N}\Theta(b_n;\lambda_n) + \sum_{k=1}^{K}\sum_{m=1}^{M}\Xi_{k,m}(s_{k,m},p_{k,m};\boldsymbol{\Lambda}_m,\nu_m) + \sum_{m=1}^{M}\nu_m p_{\max}^{\text{BS}}.
\end{aligned} \tag{22}
$$

$$
\begin{aligned}
h(\boldsymbol{\lambda},\boldsymbol{\nu}) &:= \max_{\mathbf{b},\bar{\mathbf{s}},\bar{\mathbf{p}}}\Omega(\mathbf{b},\bar{\mathbf{s}},\bar{\mathbf{p}};\boldsymbol{\lambda},\boldsymbol{\nu}) \\
&= \sum_{n=1}^{N}\overbrace{\max_{b_n}\Theta(b_n;\lambda_n)}^{\text{Subproblem 1}} + \underbrace{\sum_{k=1}^{K}\max_{\mathbf{s}_k}\sum_{m=1}^{M}\overbrace{\max_{p_{k,m}}\Xi_{k,m}(s_{k,m},p_{k,m};\boldsymbol{\Lambda}_m,\nu_m)}^{\text{Subproblem 2}}}_{\text{Subproblem 3}} + \sum_{m=1}^{M}\nu_m p_{\max}^{\text{BS}}
\end{aligned} \tag{23}
$$

1) Subproblem 1 (throughput calculation): Subproblem 1 is defined for each MS. For MS n, subproblem 1 aims to find the throughput b_n for given λ_n. That is,

$$\max_{b_n} \quad \Theta(b_n;\lambda_n) = U(b_n) - \lambda_n b_n \tag{24}$$

$$\text{s.t.} \quad b_n \geq 0. \tag{25}$$

Let $b_n^*(\lambda_n)$ be the solution of subproblem 1. From (8), we can easily find the solution as

$$b_n^*(\lambda_n) = \operatorname*{argmax}_{b\geq 0}\{U(b) - \lambda_n b\} = \lambda_n^{-1/\zeta}. \tag{26}$$

2) Subproblem 2 (transmission power allocation): Subproblem 2 is defined for each BS on each subchannel. For BS m and subchannel k, we decide the transmission power $p_{k,m}$ by solving subproblem 2 when the subchannel allocation indicator (i.e., $s_{k,m}$) and the Lagrange multipliers (i.e., $\boldsymbol{\Lambda}_m$ and ν_m) are given. Subproblem 2 is defined as in (27).

Let $p_{k,m}^*(s_{k,m};\boldsymbol{\Lambda}_m,\nu_m)$ denote the solution of this problem. It is obvious that $p_{k,m}^*(0;\boldsymbol{\Lambda}_m,\nu_m) = 0$. Since subproblem 2 is a convex optimization problem with one scalar variable, we can derive $p_{k,m}^*(1;\boldsymbol{\Lambda}_m,\nu_m)$ by using the bisection method (as given in Fig. 4). After the algorithm terminates, $(x_L + x_H)/2$ indicates $p_{k,m}^*(1;\boldsymbol{\Lambda}_m,\nu_m)$ within the error of $\epsilon/2$. This method uses the derivative of $\Xi_{k,m}(1,p_{k,m};\boldsymbol{\Lambda}_m,\nu_m)$ with respect to $p_{k,m}$. The calculation of this derivative involves numerical integration to evaluate the derivative of the average data rate in (4). For numerical integration, we use the Trapezoidal method [28, p. 216] with a uniform grid. Since we can calculate $\{\prod_{i\in\mathcal{N}_{\beta_n},i\neq n}F_{\alpha_{k,i}}(x)\}\cdot f_{\alpha_{k,n}}(x)$ for all grid points prior to running the bisection method, the complexity of numerical integration for an MS is only of the order of the number of the grid points of the Trapezoidal method.

1: $x_L \leftarrow 0$, $x_H \leftarrow \min\{D_{k,m}, p_{\max}^{\text{BS}}\}$
2: **while** $x_H - x_L > \epsilon$ **do**
3: $\quad x_M \leftarrow (x_L + x_H)/2$
4: $\quad y \leftarrow \left.\frac{\partial\Xi_{k,m}}{\partial p_{k,m}}\right|_{p_{k,m}=x_M}$
5: $\quad$ **if** $y > 0$ **then**
6: $\quad\quad x_L \leftarrow x_M$
7: $\quad$ **else**
8: $\quad\quad x_H \leftarrow x_M$
9: $\quad$ **end if**
10: **end while**

Fig. 4. Bisection method to find the optimal transmission power.

3) Subproblem 3 (subchannel allocation): Let $\Xi_{k,m}^*(s_{k,m};\boldsymbol{\Lambda}_m,\nu_m)$ be the optimal value of subproblem 2. Given $\Xi_{k,m}^*(s_{k,m};\boldsymbol{\Lambda}_m,\nu_m)$ for $s_{k,m} = 0,1$ and $m = 1,\ldots,M$, subproblem 3 is formulated to find the subchannel allocation indicators of all BSs for subchannel k:

$$
\begin{aligned}
\max_{\mathbf{s}_k} \quad & \textstyle\sum_{m=1}^{M}\Xi_{k,m}^*(s_{k,m};\boldsymbol{\Lambda}_m,\nu_m) \\
= \sum_{m=1}^{M} \quad & \max_{p_{k,m}}\Xi_{k,m}(s_{k,m},p_{k,m};\boldsymbol{\Lambda}_m,\nu_m)
\end{aligned} \tag{29}
$$

$$\text{s.t.} \quad \textstyle\sum_{m\in\mathcal{C}_a}s_{k,m} \leq 1, \quad \forall a = 1,\ldots,A \tag{30}$$

$$s_{k,m} \in \{0,1\}, \quad \forall m = 1,\ldots,M. \tag{31}$$

$$\max_{p_{k,m}} \quad \Xi_{k,m}(s_{k,m}, p_{k,m}; \mathbf{\Lambda}_m, \nu_m) = \sum_{n \in \mathcal{N}_m} \lambda_n r_{k,n}(s_{k,m}, p_{k,m}) - \nu_m p_{k,m} \tag{27}$$

$$\text{s.t.} \quad 0 \le p_{k,m} \le s_{k,m} \cdot D_{k,m}. \tag{28}$$

This problem is a combinatorial optimization problem on the conflict graph $\mathcal{G}$. We will present an algorithm to solve this problem in Section IV-C. Let $s^*_{k,m}(\boldsymbol{\lambda}, \boldsymbol{\nu})$ denote the solution to this problem. Also, we define $p^*_{k,m}(\boldsymbol{\lambda}, \boldsymbol{\nu})$ as the solution to subproblem 2 when the subchannel allocation indicator is $s^*_{k,m}(\boldsymbol{\lambda}, \boldsymbol{\nu})$, that is, $p^*_{k,m}(\boldsymbol{\lambda}, \boldsymbol{\nu}) = p^*_{k,m}(s^*_{k,m}(\boldsymbol{\lambda}, \boldsymbol{\nu}); \mathbf{\Lambda}_m, \nu_m)$. Then, $s^*_{k,m}(\boldsymbol{\lambda}, \boldsymbol{\nu})$ and $p^*_{k,m}(\boldsymbol{\lambda}, \boldsymbol{\nu})$ are the optimal subchannel allocation indicator and the optimal transmission power, respectively, when the Lagrange multipliers $\boldsymbol{\lambda}$ and $\boldsymbol{\nu}$ are given.

4) Dual Problem: The dual problem is to find the Lagrange multipliers minimizing the dual function. That is,

$$\min_{\boldsymbol{\lambda}, \boldsymbol{\nu}} \quad h(\boldsymbol{\lambda}, \boldsymbol{\nu}) \tag{32}$$

$$\text{s.t.} \quad \boldsymbol{\lambda} \succeq \mathbf{0}, \ \boldsymbol{\nu} \succeq \mathbf{0} \tag{33}$$

where "$\succeq$" denotes a component-wise inequality and $\mathbf{0}$ is a vector with all zero components. The optimal solutions of the dual problem are denoted by $\boldsymbol{\lambda}^* := (\lambda^*_n)_{n=1,\ldots,N}$ and $\boldsymbol{\nu}^* := (\nu^*_m)_{m=1,\ldots,M}$.

To solve the dual problem, we use the projection subgradient method [29]. This method iteratively updates the Lagrange multipliers until it converges to the optimal solution. Let $\boldsymbol{\lambda}^{(i)} := (\lambda^{(i)}_n)_{n=1,\ldots,N}$ and $\boldsymbol{\nu}^{(i)} := (\nu^{(i)}_m)_{m=1,\ldots,M}$ be the estimation of the optimal solution at ith iteration. Starting with the initial Lagrange multipliers that satisfy $\boldsymbol{\lambda}^{(0)} \succeq \mathbf{0}$ and $\boldsymbol{\nu}^{(0)} \succeq \mathbf{0}$, the projection subgradient method updates the Lagrange multipliers at ith iteration according to the following rules:

$$\lambda^{(i+1)}_n = \left[\lambda^{(i)}_n - \delta^{(i)} \cdot \left\{ \sum_{k=1}^{K} r_{k,n}(s^*_{k,\beta_n}(\boldsymbol{\lambda}^{(i)}, \boldsymbol{\nu}^{(i)}), p^*_{k,\beta_n}(\boldsymbol{\lambda}^{(i)}, \boldsymbol{\nu}^{(i)})) - b^*_n(\lambda^{(i)}_n) \right\} \right]^+ \tag{34}$$

and

$$\nu^{(i+1)}_m = \left[\nu^{(i)}_m - \delta^{(i)} \cdot \left\{ p^{\text{BS}}_{\max} - \sum_{k=1}^{K} p^*_{k,m}(\boldsymbol{\lambda}^{(i)}, \boldsymbol{\nu}^{(i)}) \right\} \right]^+ \tag{35}$$

where $[x]^+ = \max\{0, x\}$ and $\delta^{(i)}$ is the step size at the ith iteration.

If the step size satisfies $\delta^{(i)} > 0$, $\sum_{i=0}^{\infty} \delta^{(i)} = \infty$, and $\sum_{i=0}^{\infty} (\delta^{(i)})^2 < \infty$, it is guaranteed that $\boldsymbol{\lambda}^{(i)}$ and $\boldsymbol{\nu}^{(i)}$ converge to $\boldsymbol{\lambda}^*$ and $\boldsymbol{\nu}^*$, respectively. Alternatively, we can also use the constant step size, which makes $\boldsymbol{\lambda}^{(i)}$ and $\boldsymbol{\nu}^{(i)}$ converge to within some range of $\boldsymbol{\lambda}^*$ and $\boldsymbol{\nu}^*$. As $\boldsymbol{\lambda}^{(i)}$ and $\boldsymbol{\nu}^{(i)}$ converge to the optimal Lagrange multipliers, the subchannel allocation indicator, $s^*_{k,m}(\boldsymbol{\lambda}^{(i)}, \boldsymbol{\nu}^{(i)})$, and the transmission power, $p^*_{k,m}(\boldsymbol{\lambda}^{(i)}, \boldsymbol{\nu}^{(i)})$, also converge to the optimal solutions.

1: $\mathcal{G}_S \leftarrow \mathcal{G}$, $\mathcal{G}_T \leftarrow \mathcal{G}$, $\mathcal{V}_S \leftarrow \emptyset$
2: **while** $\mathcal{G}_S \neq \emptyset$ **do**
3: **for** $m = 1$ to M **do**
4: **if** $W_m/(\eta_m(\mathcal{G}_S)+1) > W_i/(\eta_i(\mathcal{G}_S)+1)$ for all i such that v_i is within the distance of Δ from v_m **then**
5: $\mathcal{V}_S \leftarrow \mathcal{V}_S \cup v_m$
6: Remove v_m and its neighbors from $\mathcal{G}_T$
7: **end if**
8: **end for**
9: $\mathcal{G}_S \leftarrow \mathcal{G}_T$
10: **end while**

Fig. 5. Modified greedy algorithm to find the optimal subchannel allocation indicators.

C. Maximum Weighted Independent Set Problem for Inter-cell Subchannel Allocation

We solve subproblem 3 by converting it to the MWIS problem. Since we have $\Xi^*_{k,m}(0; \mathbf{\Lambda}_m, \nu_m) = 0$, the objective function of subproblem 3 can be rewritten as

$$\sum_{m=1}^{M} \Xi^*_{k,m}(s_{k,m}; \mathbf{\Lambda}_m, \nu_m) = \sum_{m=1}^{M} W_m \cdot s_{k,m} \tag{36}$$

where $W_m := \Xi^*_{k,m}(1; \mathbf{\Lambda}_m, \nu_m)$.

The constraint (30) in subproblem 3 enforces that $s_{k,i}$ and $s_{k,j}$ cannot be one at the same time if the vertices i and j are adjacent in the conflict graph $\mathcal{G}$. Therefore, the set of v_m's for which $s_{k,m} = 1$ should form an independent set in $\mathcal{G}$.[8] If we assign W_m to v_m as a weight, subproblem 3 is reduced to the MWIS problem, that targets to find the independent set in $\mathcal{G}$ with the maximum sum of weights.

The MWIS problem is known as an NP-complete problem. Among numerous algorithms to find the suboptimal MWIS, the greedy algorithm [30] is the simplest and intuitive one. We modify the greedy algorithm, as in Fig. 5, so that it can easily be implemented in a distributed way. This algorithm uses $W_m/(\eta_m(\mathcal{G})+1)$ as a metric for v_m. We define $\eta_m(\mathcal{G})$ as the degree of v_m on $\mathcal{G}$.[9] This algorithm selects v_m, adds it to $\mathcal{V}_S$, and removes its neighbors from the graph, if v_m has the highest value of the metric among the vertices within the distance of Δ from v_m. Due to the distance restriction in the metric comparison (i.e., Δ), we can reduce the control overhead of a distributed implementation. This algorithm

[8] An independent set is a set of vertices in a graph, no two of which are adjacent.

[9] The degree is the number of edges incident on a vertex.

iterates until there is no candidate vertex, and $\mathcal{V}_S$ becomes the resulting independent set. Note that this modified algorithm is the same as the original one if Δ is no less than the diameter of $\mathcal{G}$.

D. Solving the Decomposed Problems in Functional Block Structure

The decomposed problems are assigned to the separate functional blocks illustrated in Fig. 3. The fairness control block, the transmission power allocation block, and the subchannel allocation block are responsible for solving subproblems 1, 2, and 3, respectively. In addition, the projection subgradient methods for updating $\boldsymbol{\lambda}$ and $\boldsymbol{\nu}$ are carried out by the fairness control block and the transmission power control block, respectively.

In Fig. 3, we give a detailed description of the algorithms for solving the decomposed problems in the functional block structure of BS m. In this figure, we also specify the sequential order of the algorithm executions and the information exchanges during one iteration of the projection subgradient method. It is noted that each block can execute its algorithm asynchronously in order to accelerate the convergence of the Lagrange multipliers [31]. Since the subchannel allocation block works at a larger time scale than the other blocks due to inter-cell operation, the fairness control block and the transmission power control block can expedite their convergence by executing their algorithms multiple times while the subchannel allocation block executes its algorithm.

We now present the asymptotic complexity of the algorithm in each block during one iteration. The complexity of the algorithm in the fairness control block is simply calculated as $O(K \cdot |\mathcal{N}_m|)$. Let us calculate the complexity of the bisection method in the transmission power allocation block. The bisection method repeats the cycle $O(\ln(\min\{D_{k,m}, p_{\max}^{\mathrm{BS}}\}/\epsilon))$ times. In each cycle, the bisection method conducts the evaluation of the derivative of $\Xi_{k,m}(1, p_{k,m}; \boldsymbol{\Lambda}_m, \nu_m)$ with respect to $p_{k,m}$, the complexity of which is $O(|\mathcal{N}_m| \cdot J)$, if J denotes the number of the grid points in the Trapezoidal method. Since the bisection method is performed for each subchannel, the complexity of the bisection method is given as $O(K \cdot \ln(\min\{D_{k,m}, p_{\max}^{\mathrm{BS}}\}/\epsilon) \cdot |\mathcal{N}_m| \cdot J)$.

The modified greedy method in the subchannel allocation block selects multiple vertices (i.e., BSs) to be included in the independent set in a cycle. In the worst case, $O(M)$ cycles are required to find the maximum weighted independent set. In each cycle, a BS sends a control message containing K metrics to the BSs within the distance of Δ in the conflict graph. Upon receiving the messages, a BS compares its own metrics to the other BSs' metrics. This process has the complexity of the order of K times the number of BSs within the distance of Δ. For example, if we consider the hexagonal grid topology and $\Delta = 2$, the number of BSs within the distance of Δ is 19. When Δ is given, the worst-case complexity of the modified greedy method is $O(K \cdot M)$. Therefore, the overall complexity of the proposed scheme for a BS in an iteration is $O(K \cdot \ln(\min\{D_{k,m}, p_{\max}^{\mathrm{BS}}\}/\epsilon) \cdot |\mathcal{N}_m| \cdot J + K \cdot M)$ in the worst case.

The only control overhead incurred by the proposed scheme is the communication between BSs to convey K metrics for the modified greedy method in the subchannel allocation block. It is because all the functional blocks in Fig. 3 reside within a BS and the only block communicates outside the BS is the subchannel allocation block. Since BSs are connected to each other via a high-speed wired network, this overhead does not impose significant burden to the CR system.

Although it is assumed that the channel usages of PUs are fixed in the mathematical model, it does not mean that the channel usages of PUs are invariable over time in a practical sense. The proposed scheme finds a solution for a given state of PUs (i.e., the number, channel usages, and locations of PUs) as well as the MS configuration (i.e., the number, locations, and the serving BSs of MSs). Therefore, in practice, the proposed scheme has to find a new solution every time the states of PUs and MSs change.

V. Numerical Results

We present representative simulation results for the proposed scheme, and compare its performance with that of a fixed subchannel allocation scheme. The total bandwidth of the system is 10 MHz. There are total 50 subchannels (i.e., K = 50), each of which has a bandwidth of 180 kHz (i.e., W = 180 kHz). A subchannel consists of 12 subcarriers, and the subcarrier spacing is 15 kHz. The slot duration, T_S, is 0.5 ms. In a slot, there are 7 OFDM symbols. Therefore, the OFDM symbol rate is 14 kHz, and we have R = 168 kHz.

The cells are deployed in a 4-by-4 hexagonal grid topology as depicted in Fig. 2. The inter-BS distance is 1.5 km. The MSs are uniformly distributed over the entire area. The PUs are also uniformly located, and the distance between a PU-Tx and the corresponding PU-Rx is less than 30 m (i.e., $\theta_{\max}^{\mathrm{PU}} =$ 30 m). The path-loss in dB (i.e., $10 \log_{10} \rho(d)$) is given by the formula, $128.1 + 37.6 \log_{10} d$, where d is in kilometer. The standard deviation of shadow fading, σ_ψ, is 8 dB. The mean of multi-path fading, μ_ω, is 1. The noise spectral density is -174 dBm/Hz. The maximum total transmission power of a BS, $p_{\max}^{\mathrm{BS}}$, is set to 40 W. The transmission power of a PU-Tx is 200 mW. A PU uses a subchannel that is randomly selected out of 50 subchannels. Unless noted otherwise, the parameter in the utility function, ζ, is set to one. The limit on the interference to a PU-Rx, $I_{\mathrm{lim}}^{\mathrm{PU}}$, is -115 dB, unless noted otherwise. The limit on the interference violation probability, ϵ, is 0.01. The parameter in the modified greedy algorithm, Δ, is set to two.

In Fig. 6, we show the convergence of the total transmission powers of BSs and the average data rates of MSs over the iterations of the subgradient method, when the numbers of MSs and PUs are 80 and 200, respectively. For clarity of presentation, we plot the total transmission powers of two BSs and the average data rates of two MSs only. We observe that the total transmission powers of the BSs converge to the maximum total transmission power, 40 W. The average data rates of MSs also converge and it takes about 250 iterations for the network to converge to a stable state from the algorithm initialization.

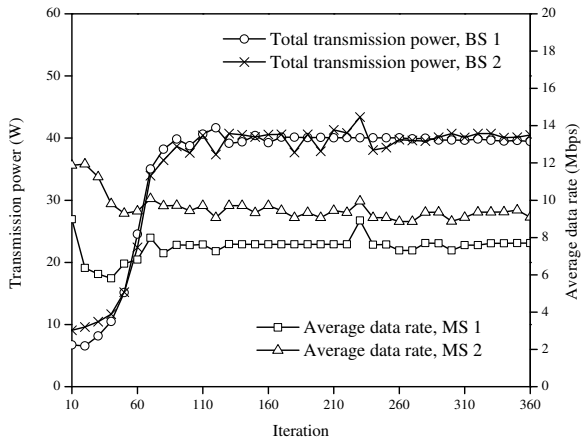

Fig. 6. Convergence of the total transmission powers of BSs and the average data rates of MSs over iterations.

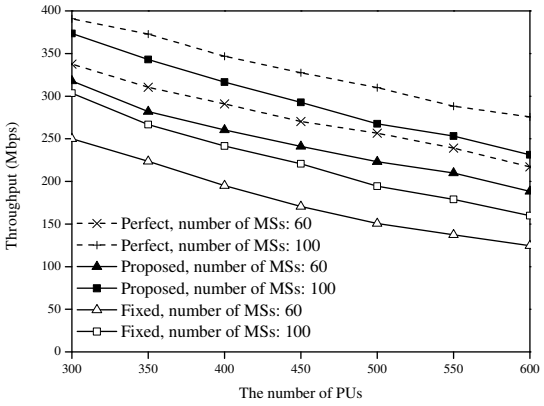

Fig. 7. Variation in total throughput of MSs with the number of PUs for the proposed scheme and the fixed scheme.

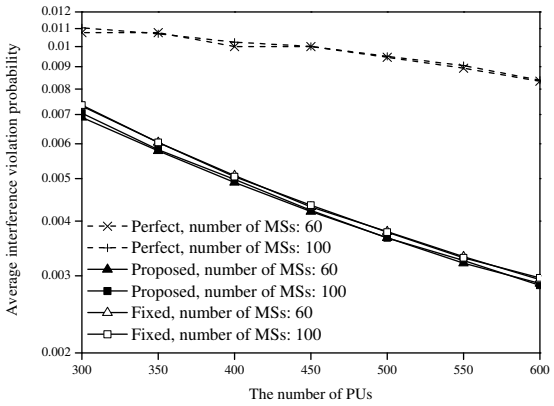

Fig. 8. Variation in average interference violation probability of PUs with the number of PUs for the proposed scheme and the fixed scheme.

In Figs. 7-8, we compare the proposed scheme with the perfect estimation scheme and the fixed subchannel allocation scheme. While the proposed scheme makes a conservative estimation of the distance to the nearest PU-Rx, we assume that the perfect estimation scheme knows the true distance to the nearest PU-Rx. The perfect estimation scheme calculates the transmission power limit based on this true distance. Except for this perfect distance estimation, the perfect estimation scheme has the same transmission power and subchannel allocation mechanism as the proposed scheme. Though the perfect estimation scheme is practically impossible to realize, it can provide an upper bound to the proposed scheme, showing how good the distance estimation of the proposed scheme is.

The fixed subchannel allocation scheme assigns the subchannels to cells with FRF of three in a fixed manner. In our simulation, we divide 50 subchannels into three subchannel groups. Subchannel group 1 includes subchannel 1 to 17, subchannel group 2 includes subchannel 18 to 34, and subchannel group 3 includes subchannel 35 to 50. Each cell statically uses one of these subchannel groups in a way that the same subchannel group is not assigned to nearby cells. Except that the subchannel allocation is predetermined, the fixed subchannel allocation scheme adopts the same resource allocation mechanism as that of the proposed scheme. That is, the fixed subchannel allocation scheme finds the optimal solution of the optimization problem (13) under the condition that $s_{k,m}$'s for all k and m are fixed to the values corresponding to the predetermined subchannel allocation. This makes the optimization problem (13) a transmission power allocation problem that can be solved by the algorithm depicted in Fig. 3 without the subchannel allocation block. The fixed subchannel allocation scheme has all the capabilities that the proposed scheme has except for the adaptive subchannel allocation, which include transmission power allocation, opportunistic scheduling, fairness control, and PU protection.

Fig. 7 plots the total throughput of MSs as a function of the number of PUs. It can be seen that the proposed scheme offers about 20% to 50% increase in the throughput compared to the fixed scheme. This performance gain over the fixed scheme comes solely from the adaptive subchannel allocation capability of the proposed scheme. As the number of PUs increases, the throughputs of both the schemes decrease since the transmission power limits tend to become lower. When the number of PUs is 600, the proposed scheme enhances the throughput by up to 50% owing to the adaptive subchannel allocation algorithm, that can assign the subchannels with high transmission power limits to cells even when PU population is very high. Compared to the perfect estimation scheme, the proposed scheme has relatively lower throughput since it conservatively estimates the distance to the nearest PU-Rx, which results in setting the transmission power limits to lower values than needed.

In Fig. 8, we present the average interference violation probability of PUs as a function of the number of PUs. Note that, even after the transmission power is decided by the proposed scheme, the interference violation probability of a PU can be nonzero since small-scale channel fading from BSs

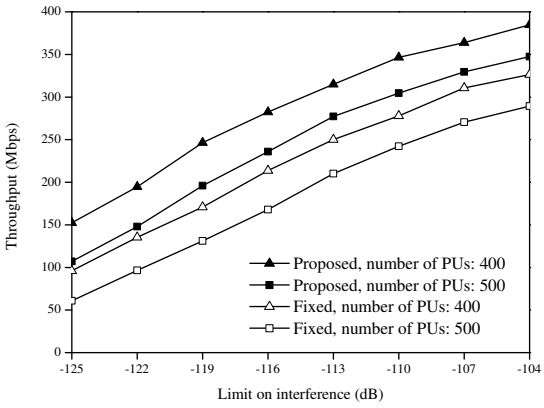

Fig. 9. Variation in total throughput of MSs with the limit on the interference to a PU-Rx, $I_{\text{lim}}^{\text{PU}}$, for the proposed scheme and the fixed scheme.

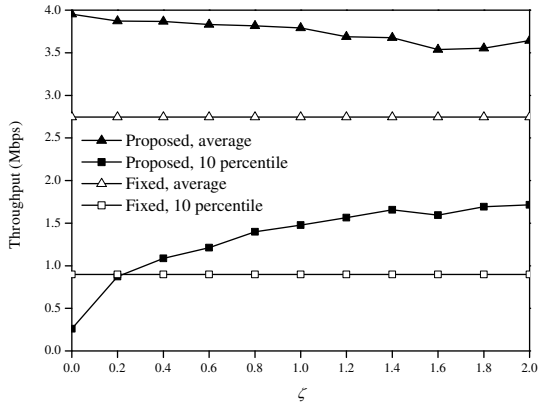

Fig. 10. Variation in average throughput and 10 percentile throughput as function of ζ for the proposed scheme and the fixed scheme.

to the PU can cause the interference to the PU to vary over time. This figure shows that the throughput enhancement of the proposed scheme over the fixed scheme is *not* at the cost of increased interference to PUs. With the proposed scheme, the interference violation probability is maintained below the target limit of 0.01. This means that the total interference to PUs is well restricted by the transmission power limits. However, the proposed scheme is overly protective of the PU due to conservative distance estimation, especially when the number of PUs is high, whereas the perfect estimation scheme keeps the interference violation probability around 0.01 regardless of the number of PUs.

Fig. 9 shows the tradeoff between the total throughput of MSs and the limit on the interference to a PU-Rx, $I_{\text{lim}}^{\text{PU}}$. The number of MSs is 80. In all simulation trials, the interference violation probabilities are maintained under 0.01. This figure shows that the limit on the interference to PUs can be lowered at the expense of the throughput of MSs. We can also see that the proposed scheme significantly outperforms the fixed scheme in terms of the throughput for the same interference to PUs.

In Fig. 10, we present the average throughput and the 10 percentile throughput as function of ζ. Recall that ζ, which is the parameter in the utility function, controls fairness among MSs. The 10 percentile throughput means that only 10% of the MSs have throughput lower than this throughput. Thus, the 10 percentile throughput is able to indicate the degree of fairness. For the simulation, the numbers of MSs and PUs are set to 80 and 400, respectively. When $\zeta = 0$, which is the case that the optimization target is the total throughput, the 10 percentile throughput of the proposed scheme is lower than that of the fixed scheme. However, if ζ is set to a value higher than 0.4, the proposed scheme guarantees more fairness than the fixed scheme, while still having higher average throughput. This means that the proposed scheme does not sacrifice fairness to enhance the system performance, as long as ζ is set to a proper value.

VI. Conclusion

We have addressed the resource allocation problem for inter-cell interference coordination in OFDMA cellular networks with the CR functionality. To solve this problem, we have proposed a subchannel and transmission power allocation scheme that adaptively assigns the radio resources considering the interference caused to the PUs. We have first formulated an optimization problem, decomposed it into multiple subproblems, and then presented the algorithms to solve these subproblems. The simulation results have shown the convergence of the proposed scheme. Also, it achieves considerably higher throughput than the fixed scheme does. The complexity of the scheme has been also analyzed.

References

[1] M. Ergen, *Mobile Broadband: Including WiMAX and LTE.* Springer, 2009.

[2] H. A. Mahmoud, T. Yucek, and H. Arslan, "OFDM for cognitive radio: Merits and challenges," *IEEE Wireless Commun. Mag.*, vol. 16, no. 2, pp. 6-14, Apr. 2009.

[3] Y. C. Liang, A. T. Hoang, and H. H. Chen, "Cognitive radio on TV bands: A new approach to provide wireless connectivity for rural areas," *IEEE Wireless Commun. Mag.*, vol. 15, no. 3, pp. 16-22, Jun. 2008.

[4] S. Chieochan and E. Hossain, "Adaptive radio resource allocation in OFDMA systems: A survey of the state-of-the-art approaches," *Wireless Communications and Mobile Computing* (Wiley), vol. 9, no. 4, pp. 513-527, Apr. 2009.

[5] G. Boudreau, J. Panicker, N. Guo, R. Chang, N. Wang, and S. Vrzic, "Interference coordination and cancellation for 4G networks," *IEEE Commun. Mag.*, vol. 47, no. 4, pp. 74-81, Apr. 2009.

[6] S. Gault, W. Hachem, and P. Ciblat, "Performance analysis of an OFDMA transmission system in a multicell environment," *IEEE Trans. Commun.*, vol. 55, no. 4, pp. 740-751, Apr. 2007.

[7] Z. Han, Z. Ji, and K. J. R. Liu, "Non-cooperative resource competition game by virtual referee in multi-cell OFDMA networks," *IEEE J. Sel. Areas Commun.*, vol. 25, no. 6, pp. 1079-1090, Aug. 2007.

[8] M. Sternad, T. Ottosson, A. Ahlen, and A. Svensson, "Attaining both coverage and high spectral efficiency with adaptive OFDM downlinks," in *Proc. IEEE VTC'03 (Fall)*, Olrando, FL, Oct. 2003, pp. 2486-2490.

[9] Huawei, *Soft Frequency Reuse Scheme for UTRAN LTE*, 3GPP Document R1-050 507, May 2005.

[10] G. Q. Li and H. Liu, "Downlink radio resource allocation for multi-cell OFDMA system," *IEEE Trans. Wireless Commun.*, vol. 5, no. 12, pp. 3451-3459, Dec. 2006.

[11] G. Bansal, J. Hossain, and V. K. Bhargava, "Optimal and suboptimal power allocation schemes for OFDM-based cognitive radio systems," *IEEE Trans. Wireless Commun.*, vol. 7, no. 11, pp. 4710-4718, Nov. 2008.

[12] R. Wang, V. K. N. Lau, L. Lv, and B. Chen, "Joint cross-layer scheduling and spectrum sensing for OFDMA cognitive radio systems," *IEEE Trans. Wireless Commun.*, vol. 8, no. 5, pp. 2410-2416, May 2009.
[13] Y. Zhang and C. Leung, "Resource allocation for non-real-time services in OFDM-based cognitive radio systems," *IEEE Commun. Lett.*, vol. 13, no. 1, pp. 16-18, Jan. 2009.
[14] F. Bernardo, R. Agusti, J. Pérez-Romero, and O. Sallent, "Dynamic spectrum assignment in multicell OFDMA networks enabling a secondary spectrum usage," *Wirel. Commun. Mob. Comput.*, vol. 9, no. 11, pp. 1502-1519, Mar. 2009.
[15] A. T. Hoang and Y. C. Liang, "Downlink channel assignment and power control for cognitive radio networks," *IEEE Trans. Wireless Commun.*, vol. 7, no. 8, pp. 3106-3117, Aug. 2008.
[16] D. P. Palomar and M. Chiang, "Alternative distributed algorithms for network utility maximization: Framework and applications," *IEEE Trans. Autom. Control*, vol. 52, no. 12, pp. 2254-2269, Dec. 2007.
[17] W. Rhee and J. M. Cioffi, "Increase in capacity of multiuser OFDM system using dynamic subchannel allocation," in *Proc. IEEE VTC'00 (Spring)*, Tokyo, Japan, May 2000, pp. 1085-1089.
[18] P. Piggin and K. L. Stanwood, "Standardizing WiMAX Solutions for Coexistence in the 3.65 GHz Band," in *Proc. IEEE DySPAN'08*, Chicago, IL, Oct. 2008, pp. 1-7.
[19] D. I. Kim, L. B. Le, and E. Hossain, "Joint rate and power allocation for cognitive radios in dynamic spectrum access environment," *IEEE Trans. Wireless Commun.*, vol. 7, no. 12, pp. 5517-5527, Dec. 2008.
[20] H. Urkowitz, "Energy detection of unknown deterministic signals," *Proceedings of the IEEE*, vol. 55, no. 4, pp. 523-531, Apr. 1967.
[21] C. J. Chen and L. C. Wang, "A unified capacity analysis for wireless systems with joint multiuser scheduling and antenna diversity in Nakagami fading channels," *IEEE Trans. Commun.*, vol. 54, no. 3, pp. 469-478, Mar. 2006.
[22] H. Fu and D. I. Kim, "Analysis of throughput and fairness with downlink scheduling in WCDMA networks," *IEEE Trans. Wireless Commun.*, vol. 5, no. 8, pp. 2164-2174, Aug. 2006.
[23] A. M. D. Turkmani, "Probability of error for M-branch macroscopic selection diversity," *Proc. IEE*, vol. 139, no. 1, pp. 71-78, Feb. 1992.
[24] N. C. Beaulieu, A. A. Abu-Dayya, and P. J. McLane, "Estimating the distribution of a sum of independent lognormal random variables," *IEEE Trans. Commun.*, vol. 43, no. 12, pp. 2869-2873, Dec. 1995.
[25] J. Mo and J. Walrand, "Fair end-to-end window-based congestion control," *IEEE/ACM Trans. Netw.*, vol. 8, no. 5, pp. 556-567, Oct. 2000.
[26] W. Yu and R. Lui, "Dual methods for nonconvex spectrum optimization of multicarrier systems," *IEEE Trans. Commun.*, vol. 54, no. 7, pp. 1310-1322, Jul. 2006.
[27] K. W. Choi, E. Hossain, and D. I. Kim. (2010, Jul.) Proof of strong duality of subchannel and power allocation problem in multi-cell OFDMA cogntive radio network. [Online]. Available: http://www.ee.umanitoba.ca/∼ekram/proof-duality.pdf
[28] K. Atkinson, *An Introduction to Numerical Analysis. 2nd ed.* New York: John Wiley & Sons, 1989.
[29] D. P. Bertsekas, *Nonlinear Programming.* Belmont, MA: Athena Scientific, 1999.
[30] S. Sakai, M. Togasaki, and K. Yamazaki, "A note on greedy algorithms for the maximum weighted independent set problem," *Discrete Applied Mathematics*, vol. 126, no. 2–3, pp. 313-322, Mar. 2003.
[31] D. P. Palomar and M. Chiang, "A tutorial on decomposition methods for network utility maximization," *IEEE J. Sel. Areas Commun.*, vol. 24, no. 8, pp. 1439–1451, Aug. 2006.

ACKNOWLEDGMENT

This research was supported in part by the Natural Sciences and Engineering Research Council (NSERC) of Canada and in part by the MKE (Ministry of Knowledge Economy), Korea, under the ITRC (Information Technology Research Center) support program supervised by the NIPA (National IT Industry Promotion Agency) (NIPA-2009-(C1090-0902-0005)).

Kae Won Choi received the B.S. degree in civil, urban, and geosystem engineering in 2001, and the M.S. and Ph.D. degrees in electrical engineering and computer science in 2003 and 2007, respectively, all from Seoul National University, Seoul, Korea. From 2008 to 2009, he was with Telecommunication Business of Samsung Electronics Co., Ltd., Korea. From 2009 to 2010, he was a postdoctoral researcher in the Department of Electrical and Computer Engineering, University of Manitoba, Winnipeg, MB, Canada. In 2010, he joined the faculty at Seoul National University of Science and Technology, Korea, where he is currently an assistant professor in the Department of Computer Science. His research interests include cognitive radio, wireless network optimization, radio resource management, and mobile cloud computing.

Ekram Hossain (S'98-M'01-SM'06) is a full Professor in the Department of Electrical and Computer Engineering at University of Manitoba, Winnipeg, Canada. He received his Ph.D. in Electrical Engineering from University of Victoria, Canada, in 2001. Dr. Hossain's current research interests include design, analysis, and optimization of wireless/mobile communications networks and cognitive radio systems (http://www.ee.umanitoba.ca/∼ekram). He serves as the Area Editor for the *IEEE Transactions on Wireless Communications* in the area of "Resource Management and Multiple Access", an Editor for the *IEEE Transactions on Mobile Computing*, the *IEEE Communications Surveys and Tutorials*, and *IEEE Wireless Communications*. Dr. Hossain has several research awards to his credit which include the University of Manitoba Merit Award in 2010 (for Research and Scholarly Activities) and the *2011 IEEE Communications Society Fred Ellersick Prize Paper Award*. He is a registered Professional Engineer in the province of Manitoba, Canada.

Dong In Kim (S'89-M'91-SM'02) received the B.S. and M.S. degrees in Electronics Engineering from Seoul National University, Seoul, Korea, in 1980 and 1984, respectively, and the M.S. and Ph.D. degrees in Electrical Engineering from University of Southern California (USC), Los Angeles, in 1987 and 1990, respectively. From 1984 to 1985, he was a Researcher with Korea Telecom Research Center, Seoul. From 1986 to 1988, he was a Korean Government Graduate Fellow in the Department of Electrical Engineering, USC. From 1991 to 2002, he was with the University of Seoul, Seoul, leading the Wireless Communications Research Group. From 2002 to 2007, he was a tenured Full Professor in the School of Engineering Science, Simon Fraser University, Burnaby, BC, Canada. From 1999 to 2000, he was a Visiting Professor at the University of Victoria, Victoria, BC. Since 2007, he has been with Sungkyunkwan University (SKKU), Suwon, Korea, where he is a Professor and SKKU Fellow in the School of Information and Communication Engineering. Since 1988, he is engaged in the research activities in the areas of wireless cellular communications. His current research interests include cooperative relaying and base station cooperation, interference management for heterogeneous networks and cognitive radio networks, cross-layer design and optimization.

Dr. Kim was an Editor for the *IEEE Journal on Selected Areas in Communications: Wireless Communications Series* and also a Division Editor for the *Journal of Communications and Networks*. He is currently an Editor for Spread Spectrum Transmission and Access for the *IEEE Transactions on Communications* and an Area Editor for Cross-layer Design and Optimization for the *IEEE Transactions on Wireless Communications*. He also serves as co-Editor-in-Chief for the *Journal of Communications and Networks*.